Cell Biochem Biophys (2014) 69:663–672
DOI 10.1007/s12013-014-9849-z

ORIGINAL PAPER

Antitumor Effect of TRAIL on Oral Squamous Cell Carcinoma using Magnetic Nanoparticle-Mediated Gene Expression

Leiying Miao · Chao Liu · Jiuyu Ge · Weidong Yang · Jinzhong Liu · Weibin Sun · Bai Yang · Changyu Zheng · Hongchen Sun · Qingang Hu

Published online: 22 February 2014

Abstract We developed a new magnetic nanovector to improve the efficiency and targeting of transgene therapy for oral squamous cell carcinoma (OSCC). Positively charged polymer PEI-modified Fe_3O_4 magnetic nanoparticles were tested as gene transfer vectors in the presence of a magnetic field. The Fe_3O_4 nanoparticles were prepared by a co-precipitation method and had good dispersibility in water. These nanoparticles modified by PEI were combined with negatively charged pACTERT-EGFP via electrostatic interaction. The transfection efficiency of the magnetic nano-gene vector with the magnetic field was determined by a fluorescence-inverted microscope and flow cytometry. The results showed significant improvement compared with the control group ($p < 0.05$). The magnetic complexes also exhibited up to 6-times higher transfection efficiency compared with commonly used PEI or lipofectin. On the basis of these results, the antitumor effect with suicide gene therapy using pACTERT-TRAIL in vitro and vivo was evaluated. In vitro apoptosis was determined with the Annexin V-FITC Apoptosis Detection Kit. The results suggested that PEI-modified Fe_3O_4 nanoparticles could mediate the killing of Tca83 cells. Furthermore, treatment with pACTERT-TRAIL delivered by magnetic nanoparticles showed a significant cytostatic effect through the induction of apoptosis in a xenograft model. This indicates that magnetic nano-gene vectors could improve the transgene efficiency for Tca83 cells and could exhibit antitumor functions with the plasmid pACTERT-TRAIL. This may be a new way to treat OSCC.

Keywords Oral squamous cell carcinoma · Nanoparticles · Polyethylenimine · Apoptosis

Introduction

Oral cancer, predominantly oral squamous cell carcinoma (OSCC), is one of the most common cancers worldwide [1]. Patients with OSCC have poor survival rates and a high incidence of metastasis. Despite recent progress in the diagnosis of and therapeutic modalities for OSCC, overall mortality rates have not improved in more than two decades [2]. New treatment strategies are needed to successfully and efficiently treat OSCC with negligible effect on normal cells as well as limited unwanted side effects.

Tumor necrosis factor-related apoptosis-inducing ligand (TRAIL) was discovered by Wiley et al. [3] and belongs to the tumor necrosis factor (TNF) cytokine family [4]. TRAIL can selectively induce strong apoptosis in a wide variety of transformed cell lines, [5] but does not affect the growth and differentiation of most normal cells and tissues [6–8]. Recent in vivo therapy experiments have

Leiying Miao and Chao Liu have contributed to this work equally.

L. Miao · C. Liu · J. Ge · W. Yang · W. Sun · Q. Hu (✉)
Institute and Hospital of Stomatology, Nanjing University Medical School, Nanjing 210008, China
e-mail: Qghu@nju.edu.cn

J. Liu · H. Sun (✉)
School of Stomatology, Jilin University, Changchun 130041, China
e-mail: drhcsun@163.com

B. Yang
State Key Laboratory of Supramolecular Structure and Materials, Jilin University, Changchun 130041, China

C. Zheng
Molecular Physiology and Therapeutics Branch, DHHS, National Institute of Dental and Craniofacial Research, NIH, Bethesda, MD, USA

demonstrated that TRAIL mediated by adenoviral vectors efficiently inhibit the xenograft tumor formation and development in nude mice [9]. Moreover, TRAIL shows a combinational effect with conventional radiotherapy or chemotherapy [10]. Although the mechanism for this cancer-specific action of TRAIL is poorly understood, it is recognized that TRAIL has the potential to become a promising antitumor therapy reagent and may provide a novel approach for cancer treatment [11, 12].

Telomeres are maintained by telomerase reverse transcriptase. Human telomerase reverse transcriptase (hTERT) is highly active in 85–90 % of human tumor cells while inactive in most human normal somatic cells [13, 14]. Approximately, 80–90 % of squamous cell carcinomas in the head and neck, including oral carcinoma, are also positive for telomerase activity [15]. Therefore, the hTERT promoter was considered as a tumor-specific promoter. Using the hTERT promoter as a tumor-specific promoter to targeted cancer cells can restrict or limit unwanted side effects. In previous studies, we used adenoviral transduction of human TRAIL driven by a tumor-specific promoter to induce apoptosis in SACC-83 cells in vitro. We also inhibited tumor growth in vivo, which used tumor-specific promoter hTERT to drive antitumor gene TRAIL expression selectively in cancer cells [16].

Recently, substantial interest has been directed toward nanoparticles with multifunctional properties due to their novel properties in promising medical applications [17–19]. Nano- or microparticles can offer a relatively large specific surface for chemical binding, and they can provide conjugation to various ligands such as drugs DNA, among other properties [20]. Magnetic nanoparticles are a special kind of nanoparticle and have been used in various areas. One of the rapidly developing applications in recent years is in the biologically related areas, for example magnetically targeting drug delivery and rapid biological separation [21–29]. Magnetic nanoparticles can be combined with DNA through a noncovalent bond, using a magnetic field to improve the efficiency and target [30–38]. This suggests a very promising future for gene therapy. We used an alkaline co-precipitation method to obtain PEI^{+}-modified Fe_3O_4 nanoparticles. The amine groups on the shell of nanoparticles can be combined electrostatically with the phosphate radical on the surface of DNA to form the magnetic and DNA nanocomposite particles by static action. The nanocomposite particles could be combined with DNA for magnetically targeting DNA delivery. The polymer PEI can protect the DNA from being digested in endosomes due to their buffer capacity via the so-called "proton sponge mechanism" [39].

We used PEI-modified Fe_3O_4 nanoparticles to mediate transfection of OSCC by human-TRAIL gene driven with a hTERT tumor-specific promoter inducing apoptosis to observe its antitumor function in vitro and in vivo.

Materials and Methods

Material and Instrumentation

The following materials were used directly without further treatment: Iron(II) chloride tetrahydrate (Sigma-Aldrich), Iron(III) chloride hexahydrate (Sigma-Aldrich), PEI, 25 kDa, branched (PEI-25Br; Sigma-Aldrich), Annexin V-FITC Apoptosis Detection Kit (BD company), lipofectin (Invitrogen), RPMI 1640 medium, fetal bovine serum, 0.05 % trypsin–EDTA (Invitrogen), pACTERT-EGFP, pACTERT-TRAIL (gift of Prof. Zheng, NIH), human tongue squamous cell carcinoma cell line Tca83 (gift of Prof. Li, Peking university school of stomatology), and Nd–Fe–B magnet (20 × 10 × 5 mm, magnetic research center of Jilin university).

Transmission electron microscopy (TEM) photographs were recorded with a JEOL-2010 electron microscope operating at 200 kV. Scanning electron microscopy (SEM) photographs were recorded with a JEOL FESEM 6700F electron microscope with primary electron energy of 3 kV, and samples were sputtered with a layer of Pt (2- to 3-nm thickness). Other equipment used included an IX51 Fluorescence-inverted microscope by OLYMPUS and flow cytometry (BD Company). The iron content of the magnetic nanoparticle was determined spectrophotometrically by complexation with 1,10-phenanthroline. Fourier transformation-IR (FT-IR) spectra of suspensions were obtained using a FT-IR spectrophotometer (Avatar 360, Nicolet).

Construction of Plasmids

Plasmids pACTERT-EGFP and pACTERT-TRAIL were constructed as previously described [16].

Synthesis of PEI-Modified Fe_3O_4 Nanoparticles

The formulation procedure of PEI-modified iron oxide nanoparticles was taken from a previous publication [40]. Briefly, 1.352 g of $FeCl_3{\cdot}6H_2O$ [Iron(III) chloride hexahydrate, Sigma-Aldrich] and 0.497 g of $FeCl_2{\cdot}4H_2O$ [Iron(II) chloride tetrahydrate, Sigma-Aldrich] were mixed, dispersed in deionized water (30 ml) by ultrasound under a flow of nitrogen, and cooled to 2–4 °C. Then, 10 ml water solution containing 2.5 ml ammonium hydroxide and 0.5 g 25 kDa branched PEI (Sigma-Aldrich) was quickly added and rapidly stirred. Thereafter, the mixture was heated to 80 °C for 2 h, then cooled to room temperature, and stirred for 1 h under ambient conditions. The precipitate was washed twice with deionized water. The product was sonicated for 5 min and was dialyzed extensively against water to remove any excess unbound PEI. The concentration of iron in the nanoparticles was 70 mg/ml, which was

measured spectrophotometrically by complexation with 1,10-phenanthroline.

Particle Size and ξ-Potential Measurement

The size and morphology of PEI-modified Fe_3O_4 nanoparticles were observed by SEM. The average hydrodynamic diameter and the ξ-potential of the particles were determined by dynamic light scattering (DLS) at 25 °C. The complexes from the 0.75 optimal ratio of PEI-modified iron oxide nanoparticles and plasmid DNA were used for this experiment (see next section for detailed procedure). Then, the DNA magnetic complex was diluted by a PBS solution to 1 ml prior to measurement.

Cell Culture

The Tca83 cell culture was maintained in RPMI 1640 medium, with 10 % fetal bovine serum (FBS), penicillin (10^5 units/liter), and streptomycin (100 mg/l) in a 5 % CO_2 incubator at 37 °C.

Determination of the Transfection Efficiency for Tca83 in Vitro

Tca83 cells were seeded at a density of 1×10^5 cells/well in a 12-well plate with 2 mL RPMI 1640 medium containing 10 % FBS for 24 h and replaced with fresh 1640 medium without FBS 1 h prior to transfection.

To evaluate the transfection efficiency of PEI-modified iron oxide nanoparticles, we compared PEI-modified iron oxide nanoparticles with PEI or lipofectin (Invitrogen). The PEI-modified iron oxide nanoparticles plus the pACTERT-EGFP or pACTERT-TRAIL complex, i.e., magnetic complex-EGFP or magnetic complex-TRAIL, was added to the culture with a Nd–Fe-B magnet ($20 \times 10 \times 5$ mm; a gift from the magnetic material research center at Jilin University, China). The plate was directly put on the Nd–Fe–B magnet for 1 h at 37 °C in a humidified 5 % CO_2 atmosphere. Then, plates were incubated at 37 °C in a humidified 5 % CO_2 atmosphere for an additional 5 h and subsequently changed with 1640 medium containing 10 % FBS at 37 °C in a humidified 5 % CO_2 atmosphere for 12 h. The optimal ratio of PEI-modified iron oxide nanoparticles and plasmid DNA is 0.75 by weight (μg). The PEI transfection used the optimal N/P ratios, PEI/DNA at N/P ratio of 8. The lipofectin was transfected as the direction. After 12 h post-transfection, transfected EGFP positive cells were counted under an OLYMPUS inverted fluorescence microscope, and transfection efficiency was determined using flow cytometry (BD Company).

Cell Viability Assay

Cell viability assay were carried out after transfections of pACTERT-TRAIL plasmid mediated by PEI-modified Fe_3O_4 nanoparticles in Tca83 cells. The optimal ratios of the DNA magnetic complex as determined by the transfection efficiency were used. Tca83 cells were seeded in a 96-well plate (5×10^4 cells/well) and cultured 24 h in 200 μL 1,640 containing 10 % FBS, then transfected with pACTERT-TRAIL or pACTERT-EGFP plasmid mediated by PEI-modified Fe_3O_4 nanoparticles with a magnet under the plate. Viability was determined using a 3-(4,5)-dimethylthiahiazol-2-y1)-2,5-diphenyltetrazolium bromide (MTT) assay (Sigma, St. Louis, MO, USA) every 2 d. The relative cell viability was calculated as cell viability (%) = (OD490 (experiment)/OD490 (control)) × 100. PEI and lipofectin were used as control.

In vitro apoptosis was determined with an Annexin V-FITC Apoptosis Detection Kit (Abcam Inc., Cambridge, MA, USA). Tca83 cells were plated in 100-mm plates (1×10^6 cells/plate) and transfected with pACTERT-TRAIL. After 72 h, cells were harvested, washed twice with PBS, and stained with Annexin V-FITC and propidium iodide (PI). Analysis of Annexin V-FITC binding was determined by flow cytometry ($Ex = 488$ nm; $Em = 530$ nm) using FITC signal detector and PI staining by the phycoerythrin emission signal detector.

Animal Experiments

Animal experiments were approved by the Jilin University Animal Care and Use Committee. Twenty male Balb/c nude mice (CAnN.Cg-Foxnl^{nu}/Crl) (4- to 6-week old) from Shanghai SLAC Laboratory Animal CO, China were used to create subcutaneous tumors by injecting Tca83 cells (2.0×10^6/mouse) into the dorsal flank. After tumor diameters reached about 5 mm, mice were randomly divided into two groups ($n = 10$). Each group was administered either PEI-modified Fe_3O_4 nanoparticles, pACTERT-TRAIL, or PBS by intratumoral injection with an insulin syringe needle (28 gage; BD). 7.5 μg of PEI-modified iron oxide nanoparticles and 10 μg of pACTERT-hTRAIL were diluted in 50 μl of PBS, respectively, for 10 min. Next, the two components were mixed together for 20 min, and this mixture was administered into the tumor. Mice were anesthetized with ketamine (60 mg/kg) and xylazine (8 mg/kg) intramuscularly. A Nd–Fe–B magnet ($20 \times 10 \times 5$ mm) was held on the skin of the tumor area for 20 min. A total of 3 injections were given once every 3 days. The size of the tumor was measured every 3 days and its volume calculated ($a \times b^2 \times 0.5$; a: largest diameter, b: smallest diameter). Animals were observed for 32 days. All animals were treated in a humane manner. To detect apoptotic cells, a standard terminal deoxynucleotidyl

transferase-mediated dUTP nick end labeling (TUNEL) assay was performed on formalin-fixed paraffin-embedded tissues according to the manufacturer's recommendations (S7101; Chemicon International, Inc., CA, USA). The number of positive cells in 1,000 tumor cells within 4–6 microscopic fields at ×200 magnification was counted.

Reverse Transcription-Polymerase Chain Reaction (RT-PCR) Assay

72 h following transduction cells were harvested, and total RNA was extracted using Trizol Reagent (Invitrogen). cDNA was synthesized with the reverse transcriptase (Invitrogen) and amplified with Taq DNA polymerase (Invitrogen) and amplicon human TRAIL-S, 5′-CCCATC-GATGGGATGACCTCTG AGGAAACC-3′ and TRAIL-A, 5′-CTAGTCTAGACTAGTTAGCCAACTA AAA A-3', and human GAPDH amplicon with GAPDH-L,5′-ACC ATAGCAGGGACAAGGTG-3′ and GAPDH-R,5′-GTGTC TGGAGCTAGGCTTGG-3'.

Statistical Analysis

Statistical analyses were carried out using SigmaStat version 2.0 (SPSS, Inc, Chicago, IL, USA). Unless stated otherwise, all experiments were performed in triplicate, and results are presented as mean values ± standard error. ANOVA testing was employed to determine the statistical significance with $p < 0.05$.

Results and Discussion

The Characterization of PEI-Modified Fe_3O_4 Nanoparticles

We used an alkaline co-precipitation method to obtain PEI-modified Fe_3O_4 nanoparticles. TEM micrographs show the morphologies of magnetite Fe_3O_4 nanoparticles (Fig. 1a) and PEI-modified Fe_3O_4 nanoparticles (Fig. 1b). It can be seen that Fe_3O_4 nanoparticles were solid quasi microspheres

Table 1 Particle size and ξ-potential measurement

	Size	ξ-potential (mV)
Fe_3O_4 nanoparticles	29.0 ± 6	−26.7 ± 1.6
PEI-modified Fe_3O_4 nanoparticles	79.6 ± 25	46 ± 0.5
PEI^+-DNA	310.7 ± 4	14.4 ± 3
DNA magnetic complex	218.2 ± 55	28.3 ± 2

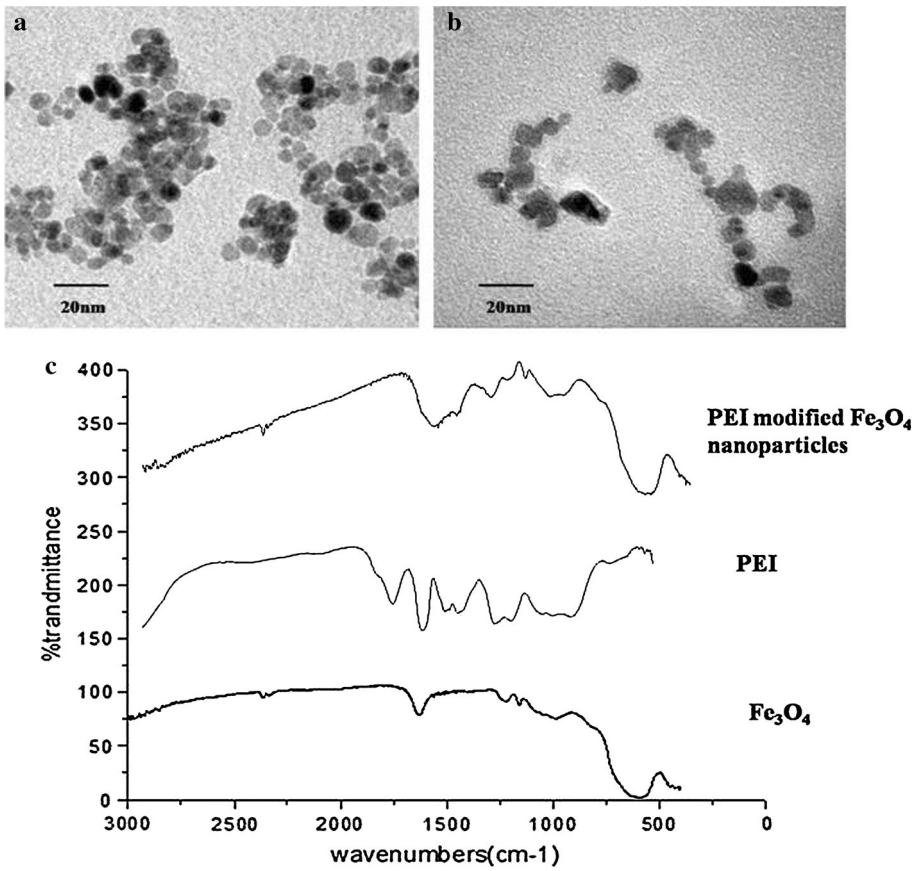

Fig. 1 TEM micrographs and FT-IR spectra. **a** Fe_3O_4 nanoparticles. **b** PEI-modified Fe_3O_4 nanoparticles. **c** FT-IR spectra of PEI-modified iron oxide nanoparticles, PEI, and Fe_3O_4 nanoparticles

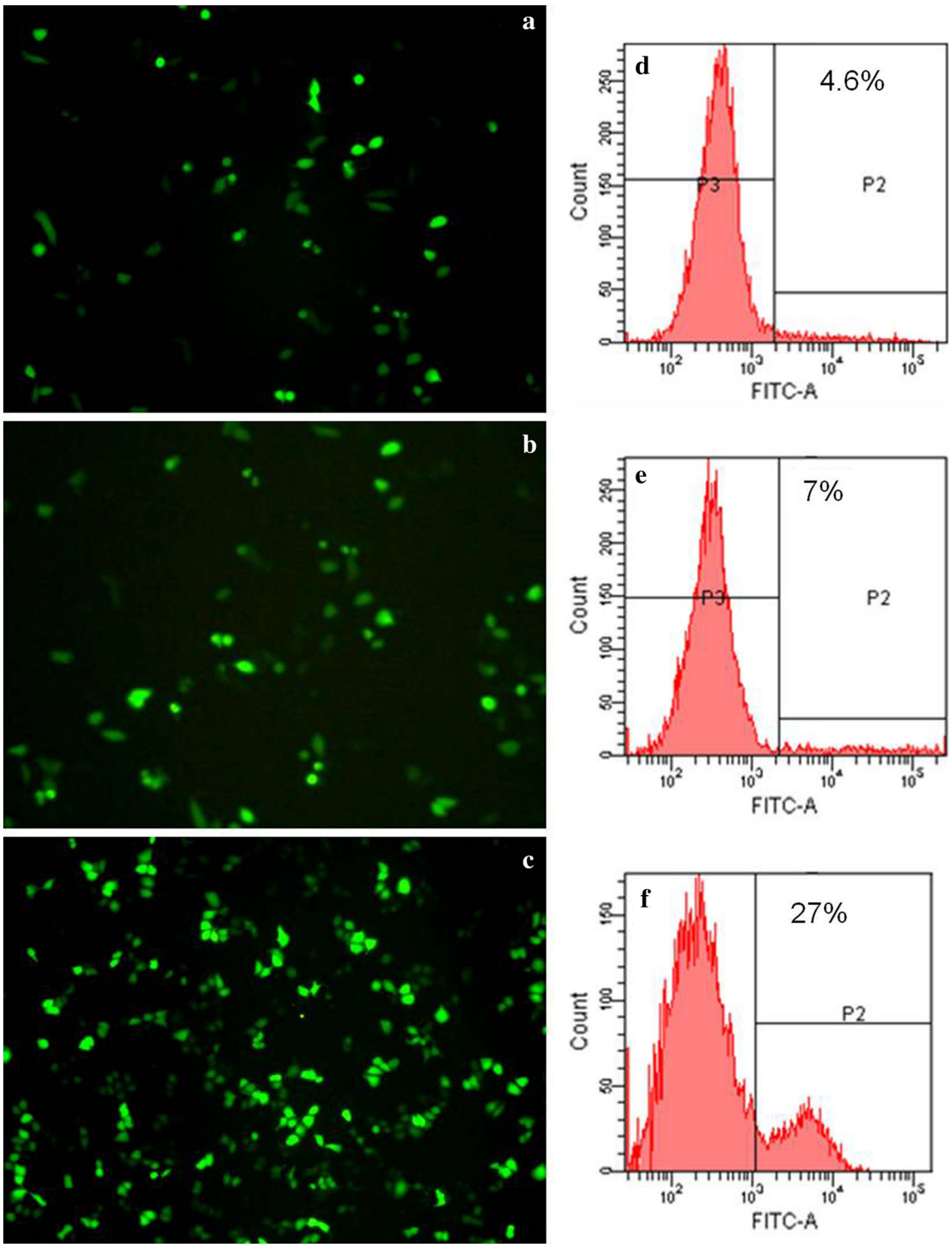

Fig. 2 Comparison of transfection efficiency between magnetic complex-EGFP, PEI, and lipofectin methods using Tca83 cells and EGFP from plasmid pACTERT-EGFP as a reporter gene. **a** EGFP expression from PEI transfection. **b** EGFP expression from lipofectin transfection. **c** EGFP expression from magnetic complex-EGFP with a Nd–Fe–B magnet underneath the plate. **d** Flow cytometry assay of PEI transfection. **e** Flow cytometry assay of lipofectin transfection. **f** Flow cytometry assay of magnetic complex-EGFP transfection with a Nd–Fe–B magnet underneath the plate

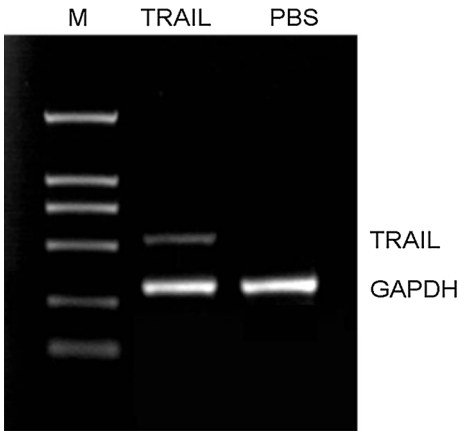

Fig. 3 Expression of hTRAIL by RT-PCR. The total RNAs were extracted from the Tca83 cells which were transfected with pACT-ERT-TRAIL plasmid mediated by PEI-modified Fe_3O_4 nanoparticles under magnetic field. GAPDH was mRNA internal control. *M* means DNA marker

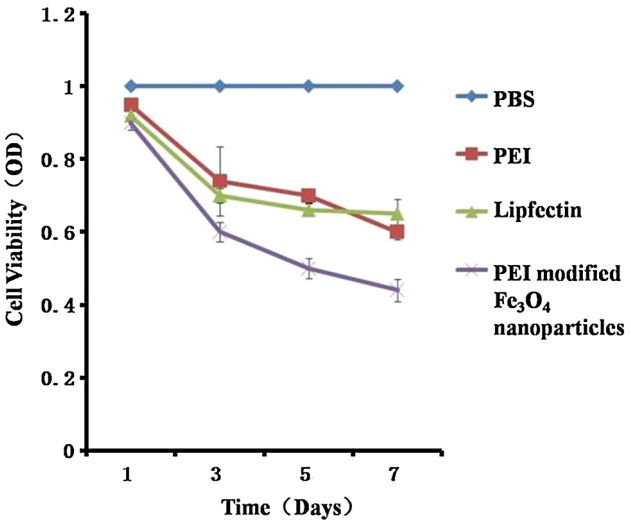

Fig. 4 Cell viability determined by MTT assay and apoptosis assay. There was a significant difference between PBS and magnetic complex–TRAIL-treated group with a Nd–Fe–B magnet ($p < 0.05$)

with an average diameter of 10 nm, and had some agglomerations (Fig. 1a). The PEI-modified magnetite nanoparticles contained a thin layer of polymer shell on the surfaces of the particles (Fig. 1b). The PEI-modified Fe_3O_4 nanoparticles had a better dispersibility than Fe_3O_4 nanoparticles in water. These nanoparticles could be quickly separated from solution using a magnet and well dispersed in water again. Since DNA is a highly anionic polyelectrolyte, the plasmids cannot combine with negative Fe_3O_4 nanoparticles because of the electrostatic repulsion, unless the surfaces of negative particles are modified by positive charges. After modification with the polyoxocations PEI, the surfaces of particles show positive charges. The amine groups on the shells of nanoparticles can combine with the phosphate radicals of DNA to form Fe_3O_4 and DNA nanocomposite particles by electrostatic action. Table 1 shows the size and ξ-potential of these nanoparticles. The ξ-potential of Fe_3O_4 was -26.7 ± 1.6 mV at pH 7.0 due to the abundant OH ions on their surfaces. After Fe_3O_4 was modified with PEI, the ξ-potential of nanoparticles changed to $+46 \pm 0.5$ mV at pH 7.0 because of the increase of the positive charges group $-NH^{4+}$ coming from PEI on the surfaces of nanoparticles. The difference in ξ-potential between PEI-modified Fe_3O_4 nanoparticles and DNA magnetic complex ($p < 0.05$) indicated that many positive charges on the surface of PEI-modified Fe_3O_4 nanoparticles bonded with the negative charges of plasmid. The iron content of the nanoparticles was 70 mg/ml, which was determined spectrophotometrically by complexation with 1,10-phenanthroline. The positive charge of the DNA magnetic complex will be more helpful for the attachment of vectors on the cell membrane, since the cell surface is slightly negatively charged. Generally, a positive surface provides a stronger interaction with the cells, leading to a faster cellular uptake compared with neural and negative surfaces, so the positively charged surface of composites is very important for cellular internalization [38].

FT-IR spectra of the PEI-modified Fe_3O_4 and Fe_3O_4 nanoparticles are shown in Fig. 1c. It shows the characteristic absorption peak of Fe_3O_4 at 576 cm^{-1}. The PEI characteristic peaks are found at 2,830 and 2,940 cm^{-1} due to the stretching vibration of the C–H bond. The IR spectrum of PEI-modified Fe_3O_4 nanoparticles showed the absorption peaks of Fe_3O_4 and PEI at 576 cm^{-1} (Fe_3O_4), 3,470 cm^{-1} (–OH), and 2,830 and 2,940 cm^{-1} ($-CH_2-$). By comparing the absorption peaks of PEI, Fe_3O_4 nanoparticles, and PEI-modified Fe_3O_4 nanoparticles, the PEI-modified Fe_3O_4 nanoparticles can be identified.

Determination of the Transfection Efficiency for Tca83 in Vitro

The co-precipitation technique likely is the simplest and most efficient chemical pathway to obtain magnetic particles. We added the polymer PEI to the alkaline solution, so the coating takes place simultaneously while the iron oxide core formed. This procedure usually generates smaller sizes of magnetic particle [39]. The smaller magnetic iron oxide particles are more quickly internalized with a final larger uptake dosage [41].

Transfection efficiency of PEI-modified Fe_3O_4 nanoparticles was compared with other well-established non-viral gene transfer systems, such as PEI polyplexes and lipofectin (Fig. 2). We used a fluorescence-inverted microscope to observe the expression of EGFP, and then

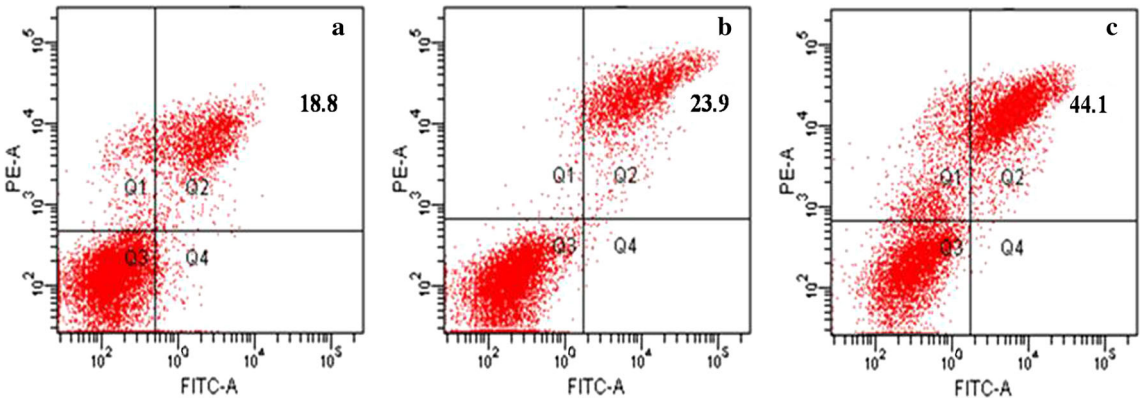

Fig. 5 Evaluation of apoptosis after Tca83 cells transfected with plasmid pACTERT-TRAIL by three methods in vitro. **a** PEI only. **b** Lipofectin. **c** Magnetic complex-TRAIL with a Nd–Fe–B magnet underneath the plate. There was no difference between PEI and lipofectin ($p > 0.05$). There was a significant difference between the magnetic complex-TRAIL with a Nd–Fe–B magnet underneath the plate and PEI or lipofectin method ($p < 0.01$). PBS was a blank control (data not shown)

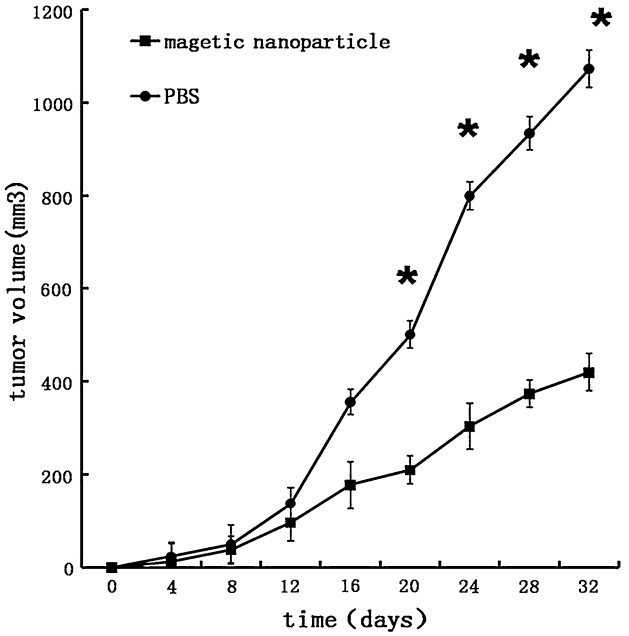

Fig. 6 Antitumor activity of hTRAIL in vivo. There were significant differences between the pACTERT-hTRAIL treated group with a Nd–Fe–B magnet and PBS ($p < 0.05$). There was no statistical difference between the two groups at the start of treatment

determined the transfection efficiency by flow cytometry. In contrast with the control group, both the amount and the brightness of the EGFP protein expression of the magnetic complexes group are the highest. The quantitative results from flow cytometry showed the same conclusion. After transfection for 12 h, the transfection efficiency for PEI-modified Fe_3O_4 nanoparticles, PEI, and the lipofectin group were 27, 4.6, and 7 %, respectively. The magnetic complexes exhibited an up to 5-fold higher transfection efficiency compared with the commonly used PEI or lipofectin, and the magnetic vectors were much superior to all other standard transfection systems. The reason may be that the magnetic field facilitated the rapid accumulation of the magnetic vectors on the cells [42].

In Vitro Cell-Specific Expression of hTRAIL

Tca83 cells were transfected with pACTERT-TRAIL plasmid mediated by PEI-modified Fe_3O_4 nanoparticles under a magnetic field at the optimum ratio determined by the transfection efficiency test. After being transfected for 72 h, cells were harvested and total RNA was used for RT-PCR (Fig. 3). We were able to detect hTRAIL (539 bp) expression.

hTRAIL Induced Apoptosis in Tca83 Cells in Vitro

We used an MTT assay to further quantify changes in cell viability. The results are displayed in Fig. 4. No difference in cell viability was measured between PEI and lipofectin. In contrast, Tca83 cells showed a substantial reduction in viability 7d following transfection with pACTERT-TRAIL magnetic complexes when compared to transfection with PEI, lipofectin, or PBS.

At the same time, we measured apoptosis of transfected cells using flow cytometry and Annexin V-FITC and PI stains. Tca83 cells which were transfected with pACTERT-TRAIL magnetic complexes showed significantly increased cell death when compared with those transfected with PEI and lipofectin ($p < 0.05$) (Fig. 5). This indicates that PEI-modified Fe_3O_4 nanoparticles had the best therapy effect in vitro.

Animal Experiments

To evaluate the antitumor effect of the DNA magnetic complexes in vivo, tumors derived from Tca83 were established in

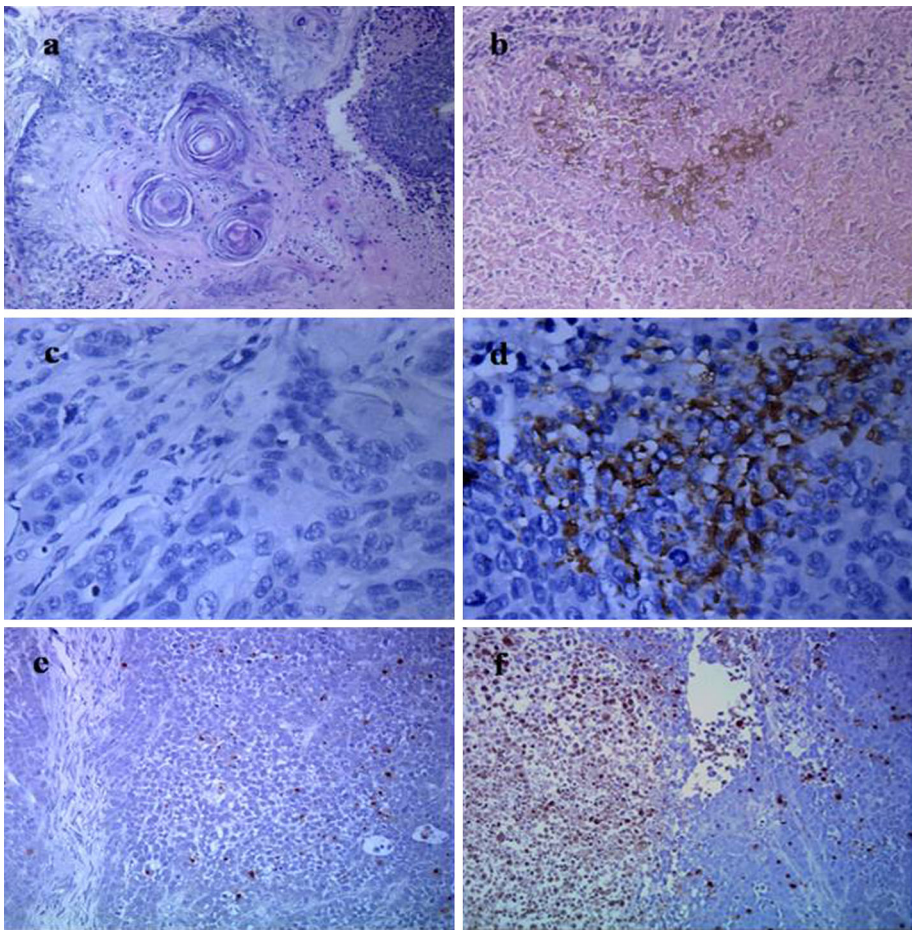

Fig. 7 Characteristics of Tca83 tumor in vivo. **a** Hematoxylin and eosin (H + E) staining from the PBS group (magnification ×100). **b** H + E staining of pACTERT-TRAIL plasmid mediated by PEI-modified Fe_3O_4 nanoparticles group (magnification ×100). **c** hTRAIL immunohistochemistry staining of PBS group (magnification ×200). **d** hTRAIL immunohistochemistry staining of PEI-modified Fe_3O_4 nanoparticles group (magnification ×200). **e** TUNEL assay of PBS group (magnification ×200). **f** TUNEL assay of pACTERT-TRAIL plasmid mediated by PEI-modified Fe_3O_4 nanoparticles group, the brown stain represented the DNA fragmentation of apoptotic cells, and the blue stain showed the nuclei stain with hematoxylin (magnification ×200). Counts of apoptotic cells from the magnetic complex–TRAIL-treated group with a Nd–Fe–B magnet were significantly different from the PBS group ($p < 0.05$)

the right flank of mice. According to the experimental protocol, the pACTERT-TRAIL magnetic complex was injected into the tumors. The magnet was left on the tumor for a total of 20 min, when tumor diameters reached about 5 mm. The mice were observed for 32 days. Tumor volumes were determined using the calculation $a \times b^2 \times 0.5$; a: largest diameter, and b: smallest diameter. The results are shown in Fig. 6. The mean tumor volumes on day 32 were 420 mm^3 for the DNA magnetic complexes treated group and 864 mm^3 for the negative control group. A significant decrease was found between the two groups on day 16 ($p < 0.01$).

Immunohistochemical analysis of tissue samples from the various groups showed that more than 73 % of tumor cells from the DNA magnetic complexes group stained positive for TRAIL, while the tumor cells from the PBS were negative (Fig. 7). TUNEL assays found a significantly higher proportion of TUNEL-positive cells in the magnetic nanoparticles group (Fig. 7). The results from these experiments support the use of magnetic nanoparticles for killing of OSCC cell in vivo.

Finding a gene transfer vector with targeting effect without side effects remains an important goal for gene therapy. In our experiment, we realized the targetted gene therapy for OSCC through three aspects. First, we used a tumor-specific promoter hTERT to control the TRAIL gene target expression in tumor tissue. Second, the hTRAIL has a tumor-specific killing activity [7]. And third, we used magnetic iron oxide nanoparticles with appropriate surface modification to target transport with an external magnetic field. Magnetic nanoparticle can be combined with plasmid to induce apoptosis of Tca83 cells in vitro and vivo, which resulted in a reduction of tumor volume. The use of magnetic nanoparticles as a gene vector for the treatment of solid tumors is relatively new. Therefore, the current study

provides a potentially novel method for the future treatment of the OSCC.

Acknowledgments This work was supported by grants from the National Natural Science Foundation of China (No: 81300852, 30672338, 30740420551 and 30830108), Jiangsu Province Natural Science Foundation of China (BK20130079), the Youth Start Fund of Nanjing City (No. 2011-19-198*), the Third Level Fund for the Young Talents in the Health Field of Nanjing City. We thank Dr. Shenglin Li at Peking University, China for a gift of the Tca83 cell line.

References

1. Shah, J. P., & Singh, B. (2006). Keynote comment: Why the lack of progress for oral cancer? *The Lancet Oncology, 7*, 356–357.
2. Gibson, M. K., & Forastiere, A. A. (2006). Reassessment of the role of induction chemotherapy for head and neck cancer. *The Lancet Oncology, 7*, 565–574.
3. Wiley, S. R., Schooley, K., Smolak, P. J., et al. (1995). Identification and characterization of a new member of the TNF family that induces apoptosis. *Immunity, 3*, 673–682.
4. Pitti, R. M., Marsters, S. A., Ruppert, S., et al. (1996). Induction of apoptosis by Apo-2 ligand, a new member of the tumor necrosis factor cytokine family. *Journal of Biological Chemistry, 271*, 12687–12690.
5. Kim, K., Fisher, M. J., Xu, S. Q., & El-Deiry, W. S. (2000). Molecular determinants of response to TRAIL in killing of normal and cancer cells. *Clinical Cancer Research, 6*, 335–346.
6. Armeanu, S., Lauer, U. M., Smirnow, I., Schenk, M., Weiss, T. S., Gregor, M., et al. (2003). Adenoviral gene transfer of tumor necrosis factor–related apoptosis inducing ligand overcomes an impaired response of hepatoma cells but causes severe apoptosis in primary human hepatocytes. *Cancer Research, 63*, 2369–2372.
7. Jacob, D., Davis, J., Zhu, H., Zhang, L., Teraishi, F., & Wu, S. (2004). Suppressing orthotopic pancreatic tumor growth with a fiber-modified adenovector expressing the TRAIL gene from the human telomerase reverse transcriptase promoter. *Clinical Cancer Research, 10*, 3535–3541.
8. Griffith, T. S., Fialkov, J. M., Scott, D. L., Azuhata, T., Williams, R. D., Wall, N. R., et al. (2002). Induction and regulation of tumor necrosis factor–related apoptosis-inducing ligand/Apo-2 ligand-mediated apoptosis in renal cell carcinoma. *Cancer Research, 62*, 3093–3099.
9. Voelkel-Johnson, C., King, D. L., & Norris, J. S. (2002). Resistance of prostate cancer cells to soluble TNF-related apoptosis-inducing ligand (TRAIL/Apo2L) can be overcome by doxorubicin or adenoviral delivery of full-length TRAIL. *Cancer Gene Therapy, 9*, 164–172.
10. Yamanaka, T., Shiraki, K., Sugimoto, K., et al. (2000). Chemotherapeutic agents augment TRAIL-induced apoptosis in human hepatocellular carcinoma cell lines. *Hepatology, 32*, 482–490.
11. Kim, C. Y., Jeong, M., Mushiake, H., Kim, B. M., Kim, W. B., Ko, J. P., et al. (2006). Cancer gene therapy using a novel secretable trimeric TRAIL. *Gene Therapy, 13*, 330–338.
12. Argiris, K., Panethymitaki, C., & Tavassoli, M. (2011). Naturally occurring, tumor-specific, therapeutic proteins. *Experimental Biology and Medicine (Maywood), 236*, 524–536.
13. Gu, J., Kagawa, S., Takakura, M., Kyo, S., Inouse, M., Roth, J. A., et al. (2000). Tumorspecific transgene expression from the human telomerase reverse transcriptase promoter enables targeting of the therapeutic effects of the Bax gene to cancers. *Cancer Research, 60*, 5359–5364.
14. Hodes, R. (2001). Molecular targeting of cancer: Telomeres as targets. *Proceedings of the National Academy of Sciences of the United States of America, 98*, 7649–7651.
15. Liao, J., Mitsuyasu, T., Yamane, K., & Ohishi, M. (2000). Telomerase activity in oral and maxillofacial tumors. *Oral Oncology, 36*, 347–352.
16. Zang, G., Miao, L., Mu, Y., et al. (2009). Adenoviral mediated transduction of adenoid cystic carcinoma by human TRAIL gene driven with hTERT tumor-specific promoter induces apoptosis. *Cancer Biology and Therapy, 8*(10), 966–972.
17. Sanvicens, N., & Marco, M. P. (2008). Multifunctional nanoparticles–properties and prospects for their use in human medicine. *Trends in Biotechnology, 26*(8), 425–433.
18. Nehilla, Barrett J., Allen, Philip G., & Desai, Tejal A. (2008). Surfactant-free, drug-quantum-dot coloaded poly(lactide-co-glycolide) nanoparticles: Towards multifunctional nanoparticles. *ACS Nano, 2*(3), 538–544.
19. Wang, Lingyan, Luo, Jin, Schadt, Mark J., & Zhong, Chuan-Jian. (2010). Thin film assemblies of molecularly-linked metal nanoparticles and multifunctional properties. *Langmuir, 26*(2), 618–632.
20. Pellegrino, T., Kudera, S., Liedl, T., Muñoz Javier, A., Manna, L., & Parak, W. J. (2005). On the development of colloidal nanoparticles towards multifunctional structures and their possible use for biological applications. *Small, 1*(1), 48–63.
21. Lee, Mei-Hwa, Thomas, James L., Ho, Min-Hsien, Yuan, Ching, & Lin, Hung-Yin. (2010). Synthesis of magnetic molecularly imprinted poly(ethylene-co-vinyl alcohol) nanoparticles and their uses in the extraction and sensing of target molecules in urine. *ACS Applied Materials and Interfaces, 2*(6), 1729–1736.
22. Mahmoudi, Morteza, Simchi, Abdolreza, Imani, Mohammad, & Hfeli, Urs O. (2009). Superparamagnetic iron oxide nanoparticles with rigid cross-linked polyethylene glycol fumarate coating for application in imaging and drug delivery. *Journal of Physical Chemistry C, 113*(19), 8124–8131.
23. Williams, P. S., Carpino, F., & Zborowski, M. (2009). Magnetic nanoparticle drug carriers and their study by quadrupole magnetic field-flow fractionation. *Molecular pharmaceutics, 6*(5), 1290–1306.
24. Liong, M., Lu, J., Kovochich, M., Xia, T., Ruehm, S. G., Nel, A. E., et al. (2008). Multifunctional inorganic nanoparticles for imaging, targeting, and drug delivery. *ACS Nano, 2*(5), 889–896.
25. Gao, Jinhao, Hongwei, Gu, & Bing, Xu. (2009). Multifunctional magnetic nanoparticles: Design, synthesis, and biomedical applications. *Accounts of Chemical Research, 42*(8), 1097–1107.
26. Mori, Kohsuke, Kondo, Yuichi, Morimoto, Shotaro, & Yamashita, Hiromi. (2008). Synthesis and multifunctional properties of superparamagnetic iron oxide nanoparticles coated with mesoporous silica involving single-site Ti oxide moiety. *Journal of Physical Chemistry C, 112*, 397–404.
27. Sun, C., Du, K., Fang, C., Bhattarai, N., Veiseh, O., Kievit, F., et al. (2010). PEG-mediated synthesis of highly dispersive multifunctional superparamagnetic nanoparticles: Their physicochemical properties and function in vivo. *ACS Nano, 4*(4), 2402–2410.
28. Jain, T., Morales, M., Sahoo, S., et al. (2005). Iron oxide nanoparticles for sustained delivery of anticancer agents. *Molecular Pharmaceutics, 2*(3), 194–205.
29. Son, S., Reichel, J., He, B., et al. (2005). Magnetic nanotubes for magnetic-field-assisted bioseparation, biointeraction, and drug delivery. *Journal of the American Chemical Society, 127*(20), 7316–7317.
30. Namgung, R., Singha, K., Yu, M. K., Jon, S., Kim, Y. S., Ahn, Y., et al. (2010). Hybrid superparamagnetic iron oxide nanoparticle-branched polyethylenimine magnetoplexes for gene transfection of vascular endothelial cells. *Biomaterials, 31*(14), 4204–4213.

31. Zheng, X., Lu, J., Deng, L., Xiong, Y., & Chen, J. (2009). Preparation and characterization of magnetic cationic liposome in gene delivery. *International Journal of Pharmaceutics, 366*(1–2), 211–217.
32. Kievit, F. M., Veiseh, O., Fang, C., Bhattarai, N., Lee, D., Ellenbogen, R. G., et al. (2010). Chlorotoxin labeled magnetic nanovectors for targeted gene delivery to glioma. *ACS Nano, 4*(8), 4587–4594.
33. Scherer, F., Anton, M., Schillinger, U., et al. (2002). Magnetofection: Enhancing and targeting gene delivery by magnetic force in vitro and in vivo. *Gene Therapy, 9*(2), 102–109.
34. Moore, A., Marecos, E., Bogdanov, A, Jr, et al. (2000). Tumoral distribution of long-circulating dextran-coated iron oxide nanoparticles in a rodent model. *Radiology, 214*(2), 568–574.
35. Kamau, W., Hassa, P., Steitz, B., et al. (2006). Enhancement of the efficiency of non-viral gene delivery by application of pulsed magnetic field. *Nucleic Acids Research, 34*(5), e40.
36. Kadota, S., Kanayama, T., Miyajima, N., et al. (2005). Enhancing of measles virus infection by magnetofection. *Journal of Virological Methods, 128*(1–2), 61–66.
37. Morishita, N., Nakagami, H., Morishita, R., et al. (2005). Magnetic nanoparticles with surface modification enhanced gene delivery of HVJ-E vector. *Biochemical and Biophysical Research Communications, 334*(4), 1121–1126.
38. Plank, C., Anton, M., Rudolph, C., et al. (2003). Enhancing and targeting nucleic acid delivery by magnetic force. *Expert Opinion on Biological Therapy, 3*, 745–758.
39. Boussif, O., Lezoualc'h, F., Zanta, M. A., Mergny, M. D., Scherman, D., Demeneix, B., et al. (1995). A versatile vector for gene and oligonucleotide transfer into cells in culture and in vivo: Polyethylenimine. *Proceedings of the National Academy of Sciences of the United States of America, 92*(16), 7297–7301.
40. Miao, L., Zhang, K., Qiao, C., Jin, X., Zheng, C., Yang, B., et al. (2013). Antitumor effect of human TRAIL on adenoid cystic carcinoma using magnetic nanoparticle-mediated gene expression. *Nanomedicine: Nanotechnology, Biology, and Medicine, 9*(1), 141–150.
41. Lee, H., Lee, E., Kim do, K., Jang, N. K., Jeong, Y. Y., & Jon, S. (2006). Antibiofouling polymer-coated superparamagnetic iron oxide nanoparticles as potential magnetic resonance contrast agents for in vivo cancer imaging. *Journal of the American Chemical Society, 128*, 7383–7389.
42. Pan, X., Guan, J., Yoo, J. W., Epstein, A. J., Lee, L. J., & Lee, R. J. (2008). Cationic lipid coated magnetic nanoparticles associated with transferring for gene delivery. *International Journal of Pharmaceutics, 358*, 263–270.